PCCP

Accepted Manuscript

ROYAL SOCIETY OF CHEMISTRY

www.rsc.org/pccp

Bimetallic Dimers Adsorbed on Defect-free MgO(001) Surface: Bonding, Structure and Reactivity

Igor A. Pašti[a],* Miloš R. Baljozović[a], Laura P. Granda-Marulanda[a], Natalia V. Skorodumova[b,c]

[a]*University of Belgrade, Faculty of Physical Chemistry, Studentski trg 12-16, 11158 Belgrade, Serbia*

[b]*Multiscale Materials Modelling, Materials Science and Engineering, School of Industrial Engineering and Management, KTH - Royal Institute of Technology, Brinellvägen 23, 100 44 Stockholm, Sweden*

[c]*Department of Physics and Astronomy, Uppsala University, Box 516, 751 20 Uppsala, Sweden*

***corresponding author:**

Dr. Igor A. Pašti, assistant professor

University of Belgrade, Faculty of Physical Chemistry

Studentski trg 12-16, 11158 Belgrade, Serbia

e-mail: igor@ffh.bg.ac.rs

Phone: +381 11 3336 628

Fax: +381 11 2187 133

Abstract

Large number of computational studies has been devoted to the investigation of monometallic clusters supported by MgO. However, practice in catalysis shows that multicomponent catalytic systems often win in catalytic performance over single component systems. In this study, the geometrical and electronic structure, stability and chemisorption properties of M1M2 metal dimers (M1, M2 = Ru, Rh, Pd, Ir, Pt) supported by defect free MgO(001) have been investigated in the framework of density functional theory. The oxygen sites of MgO(001) are the preferred adsorption sites for all the studied clusters, the majority of them adsorb parallel to the surface with metal atoms attached to two surface oxygen atoms. The energetics of M1M2+MgO(001) formation shows that the adsorption complexes are stable and benefit from metal–oxygen and metal–metal interaction. The chemisorption properties of Pd and Pt atoms in PdM2 and PtM2 dimers are studied using CO as a probe molecule. A linear relationship between the CO chemisorption and the d-band center position of the reacting atom in the dimer is observed, extending the d-band center model to the case of highly under-coordinated metal atoms supported by non-conductive material.

Keywords: MgO(001), metal dimer, adsorption, electronic structure, CO chemisorption

I. Introduction

Catalysis is a crucial part of many technological processes and its understanding at a fundamental level is a timely challenge for materials science community. Both experimental and theoretical approaches are employed to resolve crucial steps of different catalytic processes at the atomic level. Supported metal clusters are among the systems of particular interest, as they present a basis for the understanding of cluster growth, nucleation, mobility and catalytic activity.[1] In practice, the high dispersion of a catalytically active component over a suitable support increases its active surface area while low-coordinated atoms often act as active sites.[2] Increasing the dispersion one reaches the limit of single supported atoms for which the catalytic effect was also observed. For example, the work of Qiao *et al.* demonstrates that single Pt atoms supported by FeO_x nanocrystals show a high catalytic activity towards CO oxidation and preferential oxidation of CO in H_2.[3] The observed high catalytic activity of Pt atoms is due to a reduced Pt–CO bond strength, which is a consequence of Pt interaction with the FeOx support.[3] The catalytic activity of supported dimers was also demonstrated experimentally.[4, 5] Yardimci *et al.* have synthesized a MgO supported dinuclear Rh catalyst with high activity towards ethylene hydrogenation,[5] which, in fact, was 58 times more active than the atomically dispersed catalyst.[5] Therefore, supported metal atoms and dimers are not just model systems but they can find numerous practical applications.[3]

One of the most common catalyst supports is magnesium oxide, MgO.[6-9] MgO(001) surface is non-polar, easy to prepare and does not exhibit significant structural relaxation.[10, 11] Due to these properties MgO is widely used in surface science studies and one can find a large body of theoretical and experimental work accumulated over the years, in particular, for MgO(001)-supported metal clusters. Theoretical methods allow for the investigation of the

effects of cluster size and can provide insights which are often beyond the abilities of experimental methods. In particular, a significant amount of computational results on, usually, homonuclear metal dimers on MgO(001) can be found in the literature.[12-19] On the other hand, practice in catalysis shows that multicomponent catalytic systems often win in catalytic performance over single component systems. As a well known example, one might mention the bifunctional mechanism of alcohol oxidation on PtRu surface where the oxidation of intermediately formed CO (which adsorbs at the Pt sites) is promoted by the formation of adjacent Ru–OH groups.[20] Therefore, it is particularly interesting to analyze MgO-supported bimetallic clusters, which represent the smallest possible model of supported metal clusters. The knowledge gained from this kind of studies could allow us to to optimize the chemical reactivity of clusters by the adjustment of the chemical composition.[21-24] For example, Matczak investigated H_2 interaction with MgO(001) supported PdAg, PdAu, PtAg and PtAu bimetallic dimers and showed that MgO support decreases the ability of the dimers to adsorb and dissociate hydrogen molecules.[21] Florez *et al.* investigated Cu_nM (M= Ni, Pd, Pt; n = 1–4) bimetallic nanoparticles adsorbed on F_s center of MgO(001) and showed that chemical reactivity depends on the nanoparticles arrangement on the surface as well as on the type of binding atom (Cu or M).[22] Obviously, catalysis by highly undercoordinated metal atoms becomes reality, but very little is known about the electronic structure parameters that govern their reactivity. When it comes to catalysis, the interaction between the reactants and the catalysts is of crucial importance and it is vital to understand how the changes in the chemical composition and the electronic structure of catalysts determine this step. For metallic surfaces the theory is well-established, and allows for the understanding of the reactivity trends and rational design of new catalytic systems.[25] So, the question is whether some electronic structure parameters can be used to

understand the chemisorptions properties and the reactivity of a metal atom in small supported metal clusters?

Here we apply a combinatorial approach to analyze the interaction of bimetallic M1M2 (M1, M2 = Ru, Rh, Pd, Ir, Pt) dimers with defect-free MgO(001). We address the issues of their structure, electronic structure, bonding and stability on MgO(001). We also analyze the CO chemisorption properties of PdM2 and PtM2 dimers and verify the applicability of the d-band center model, proposed by Hammer and Nørskov,[25] for the case of highly undercoordinated atoms.

II. Computational methods

The performed calculations were based on Density Functional Theory (DFT) within the generalized gradient approximation (GGA) employing Perdew–Burke–Ernzerhof exchange correlation functional.[26] The calculations were done using the PWscf code of Quantum ESPRESSO distribution.[27] Ultra soft pseudopotentials were used for the treatment of core electrons. The kinetic energy cutoff for the selection of the plane-wave basis set was 28 Ry (380.8 eV) and the charge density cutoff was 16 times higher, for all the calculations. The lattice constant of 4.22 Å was obtained for bulk MgO, which is in good agreement with the experimental value of 4.21 Å.[28] The MgO (001) surface was modeled by a three layer slab with the (2×2) unit cell having eight magnesium and eight oxygen atoms per layer. The atoms in the MgO(001) slab were relaxed, except for the bottom layer, which was fixed during geometry optimization. All the geometries were optimized until the remaining forces were smaller than 10^{-3} Ry $Å^{-1}$. The integration over the irreducible edge of the Brillouin zone was done using a (2×2×1) Monkhorst-Pack grid.[29] A Gaussian smearing procedure, with the broadening of 0.007

Ry, was applied. The surface slabs were separated by a vacuum region of 12 Å. The extension of the vacuum region from 12 Å to 18 Å affected the adsorption energies by less than 0.5 meV while no effects on electronic structure descriptors discussed below was observed. Moreover, the dipole correction was added to prevent the interaction along the z direction.[30] The model used here to simulate the MgO(001) surface is described in detail in our previous work.[31]

Monomers and dimers of investigated transition metals were places on one side of MgO(001) and fully relaxed. We investigated two isomeric structures of metal dimers with respect to the MgO surface plane: parallel to the surface with M atoms attached to surface oxygens (Fig. 1, C, flat-OO), and vertical to the surface with one atom bonded to the O center (Fig 1, E, vertical-Otop).

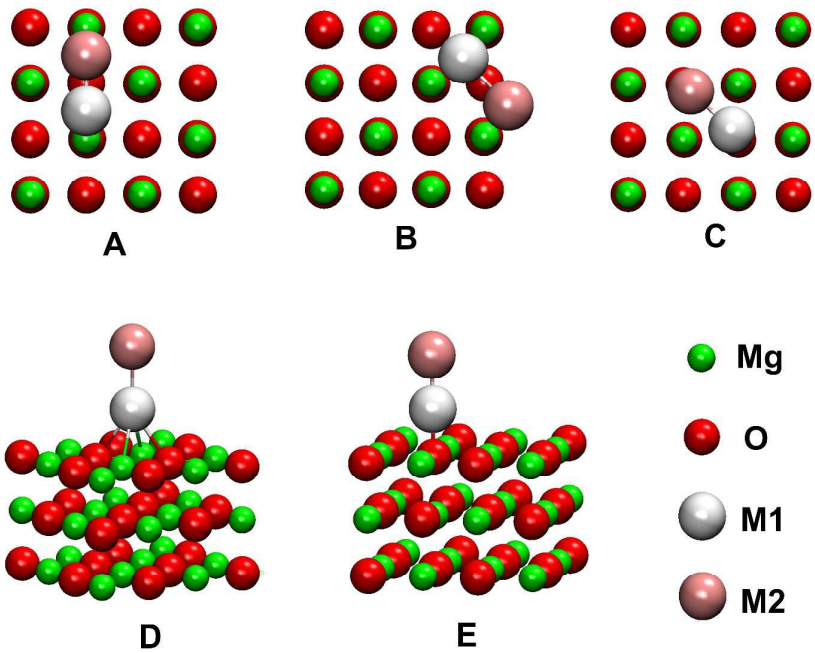

Figure 1. Initial structures for the adsorption of M1M2 dimers on defect-free Mg(001) terrace: flat-brigde-Mg (A), flat-bridge-O (B), flat-OO (C), vertical-hollow (D) and vertical-Otop (E). For each of the structures D and E there are two possibilities depending whether M1 or M2 are attached to the surface. Graphical presentations were made using VMD code.[32]

We considered different possible orientations of M1M2 dimers with respect to the MgO surface (Fig. 1), in total 5 for homonuclear dimers (M1 = M2) and 7 for heteronuclear dimers (M1 ≠ M2). Preliminary calculations showed that the 2 layers MgO(001) slab already provides an adequate description of adsorption energetics, in agreement with ref[33]. The increase of number of MgO layers to 3 changes the adsorption energies by less than 0.05eV.

In this work we study the reactivity of highly under-coordinated metal atoms. In particular, we analyzed the properties of a set of supported bimetallic dimers using CO as a probe molecule. The probe molecule was placed on top of either Pd atom in PdM2 dimer or Pt atom in PtM2 dimer and the structure was fully relaxed. For the analysis of the CO adsorption the calculations were performed using elongated cells so that the vacuum region was approximately 12 Å between the adsorbed CO molecule and the bottom of the subsequent surface slab. Our intention was to test the reactivity of a particular atom (Pd or Pt) in the dimer and link it to its electronic structure in the dimer but not to find the ground state configuration of adsorbed CO. Here we do not investigate the ways CO can approach the dimers, or a possibility that CO can simultaneously attach to the dimer and the MgO support, although such bonding is important in heterogeneous catalysis.[34-36]

The charge transfer was analyzed using the Bader algorithm[37] on a charge density grid by Henkelman *et al.*[38]

III. Results and discussion

A. Monomers and homonuclear dimers on Mg(001)

The adsorption of single metal atoms: Ru, Rh, Pd, Ir, Pt, was analyzed for the four high-symmetry adsorption sites of MgO(001): O-top, Mg-top, four-fold hollow and Mg-O bridge.

Upon complete relaxation all the metal adatoms were found to bind directly on top of the surface oxygen. The metal binding energy (E_b^M) was calculated as:

$$E_b^M = E_{MgO+M} - \left(E_{MgO} + E_M\right) \quad (1)$$

where E_{MgO+M}, E_{MgO} and E_M are the total energy of MgO(001) surface with adsorbed M, the total energy of bare MgO surface and the total energy of an isolated M atom. E_b^M refers to the spin-polarized ground state of an isolated M atom, as usually done.[39] It has earlier been discussed that spin-polarization effects in the adsorbate reference state prevail over those in the adsorption complex and that a proper spin-polarized reference state for the adsorbate results in a fair estimate of its binding energy even if spin-polarization is disregarded for the adsorption complex.[40] As an example, one can mention the work of Mineva *et al.* on Rh adsorption on MgO(001).[41] The authors have shown that for the ground state of a Rh atom adsorbed on the O site of MgO(001) the inclusion of spin polarization lowers the total energy by 0.14 eV, that agrees with our result (Table 1). However, for an isolated atom we calculated this energy difference to be 1.52 eV, which is one order of magnitude higher than that for the adsorption complex. The metal binding energies calculated without spin-polarization span from −0.75 eV (Ru) to −2.27 eV (Pt) and from −1.09 eV (Ru) to −2.27 eV (Pt) when calculated including spin-polarization (Table 1). It is important to point out that in the case of adsorbed monomers (i) spin polarization did not affect adsorption site preference and (ii) did not affect the overall trend of the calculated adsorption energies. An overall trend is an increase of E_b^M upon moving to the right and down in the Periodic Table of Elements (PTE) with Pd slightly deviating from this rule. This might be associated with the tendency of metal atoms to complete their electronic shells by charge transfer from the substrate. In the previous study of transition metal adsorption on MgO(001) performed by Neyman *et al.*, a complicated dependence of E_b^M on the element

position in the PTE was observed. In particular, it appeared that E_b^M increased along the period of the PTE being the most exothermic for the $ns^1(n-1)d^9$ elements, which was followed by a large decrease for Cu, Ag and Au.[40] As pointed out, there are three main factors affecting E_b^M: (i) adsorbates polarization at the surface, (ii) the orbital overlap of metal s(d)-states with O 2p-states, and (iii) Pauli repulsion of the filled electronic shells.

Table 1. Metal binding energies (E_b^M) for the preferential O top site and M−O bond lengths for metal adatoms on defect free MgO(001) (*d*(M–O)). The results for spin-unpolarized and spin-polarized calculations are given. The literature data for E_b^M are included for comparison

	spin-unpolarized		spin-polarized			
adatom	E_b^M **/ eV**	***d*(M–O) / Å**	E_b^M **/ eV**	***d*(M–O) / Å**	**magnetization/μ_B**	**literature**
Ru	−0.75	2.00	−1.09	2.03	4	−0.89[a]
Rh	−1.52	2.03	−1.68	2.07	1	−1.30[a] −1.59[b] −1.92[b] −2[c]
Pd	−1.35	2.10	−1.35	2.10	0	−1.35[d] −1.37[e] −1.42[a]
Ir	−1.85	1.97	−1.98	2.01	1	−1.41[a]
Pt	−2.27	1.98	−2.27	1.98	0	−1.50[f] −2.35[g] −2.35[d] −2.39[a]

[a]Reference.[40] [b]Reference.[41] [c]Reference.[42] [d]Reference.[43] [e]Reference.[44] [f]Reference.[39] [g]Reference.[45]

In spite of particular theoretical and technological importance of oxide-supported metallic particles, the adsorption of metal atoms on MgO(001) remains a subject, which is only partially covered by the available literature, where one can find a wide variety of different surface models and methodologies applied to investigate metal adsorption on MgO. The work presented by

Neyman *et al.* provides a systematic analysis of the adsorption of d-metals on MgO(001) using the cluster approach with two different GGA functionals.[40] The data obtained using BP86 functional (see Table 1) provide good overall agreement with our results reported here. However, there is a noticeable scattering of available E_b^M data for Rh and Pt on MgO(001) even in the cases where similar surface models have been used. For Pt, reported E_b^M span from −1.50 eV[39] to −2.35 eV[43] for the slab calculations. Interestingly, at the same time no large differences in adsorption geometries were found. The Pt–O bond length was previously reported to be close to 2 Å,[39] while the value of 1.98 Å was reported in ref. 43, the latter value being identical to the one presented in this work. Both Pd and Pt adsorbed at the O site of MgO(001) were found to have a non-magnetic ground state.[43] For Pd, the Pd–O distance was found to be 2.09 Å[43] that is in close agreement with our value.

Now we proceed to homonuclear dimers applying the same methodology as for adsorbed monomers. The formation energy of the M_2/MgO(001) complex was characterized by the dimer adsorption energy (E_{ads}), defined as:

$$E_{ads} = E_{MgO+M_2} - \left(E_{MgO} + E_{M_2}\right) \qquad (2)$$

where E_{MgO+M_2}, E_{MgO} and E_{M_2} are the total energy of MgO(001) surface with the adsorbed M_2 dimer, the total energy of the bare MgO surface and the total energy of the spin-polarized ground state of an isolated M_2 dimer, respectively.

The investigated homonuclear dimers preferred a parallel arrangement except for Ir and Pt, which preferred to adsorb vertically (Table 2). Some earlier work suggested a parallel orientation of the Pt_2 dimer with respect to MgO(001),[39] while a more recent one suggested that the vertical orientation is favored.[46] According to the recent literature the Pd_2 dimer prefers the parallel orientation with respect to MgO(001).[14] Our findings agree with this data. For the case of

MgO(001)-supported Pd_2 a direct experimental observation was reported. By means of the low-temperature scanning tunneling microscopy the parallel orientation of Pd_2 with respect to MgO(001) was confirmed and the estimated Pd–Pd bond length was of about 2.8 Å.[14]

Table 2. Adsorption energies (E_{ads}) of homonuclear dimers at Flat-OO and Otop sites and M−M bond lengths for homonuclear dimers on defect free MgO(001) (*d*(M–M)). The results for spin-unpolarized and spin-polarized calculations are given. For the spin-polarized calculations the magnetization of the ground state is given. In parentheses, ground state magnetization of the isolated dimer is given.

		spin-unpolarized		**spin-polarized**		
dimer	**Ads. site**	E_{ads} / **eV**	***d*(M–M) / Å**	E_{ads} / **eV**	***d*(M–M) / Å**	**Magnetization / μ_B**
Ru_2	Flat-OO	−0.98	2.32	−1.52	2.34	6(6)
	Otop	−0.88	2.11	−0.88	2.11	0(6)
Rh_2	Flat-OO	−1.19	2.38	−1.67	2.37	4(4)
	Otop	−0.62	2.24	−1.32	2.29	4(4)
Pd_2	Flat-OO	−2.08	2.82	−2.08	2.82	0(2)
	Otop	−1.17	2.51	−1.17	2.51	0(2)
Ir_2	Flat-OO	−1.12	2.36	−1.78	2.32	2(4)
	Otop	−1.45	2.23	−1.88	2.29	4(4)
Pt_2	Flat-OO	−1.59	2.56	−1.77	2.54	2(2)
	Otop	−1.71	2.38	−2.02	2.37	2(2)

The effect of spin polarization on the preferential orientation of adsorbed dimers and adsorption energies should be discussed. In the case of Pd_2, the gas phase dimer has a magnetic moment of 2 μ_B, while the ground state of an adsorbed dimer is non-magnetic.[46] It has previously been reported that the parallel orientation of Pd_2 on MgO(001) is favored by 0.94 eV over the vertical one, when spin polarization is taken into account.[46] Here we find this difference to be 0.91 eV. In

the case of the Pt dimer the magnetic moment (2 μ_B) found in the gas phase is preserved upon dimer adsorption onto MgO(001), the vertical orientation is preferred over vertical one by 0.28 eV.[46] Within the spin- polarized approach employed here this difference is 0. 25 eV, while for the spin- restricted case we found 0.12 eV. Although the effect of spin polarization is clearly visible and affects calculated E_{ads} to a noticeable extent, the trends in adsorption energies and the preference of the adsorption site is preserved (Table 2).

We observed that for all dimers except Pd_2 the ground state magnetization matches the one of the isolated dimer. These magnetic solutions agree with previously reported ones.[46] However, for the Ru_2 and Ir_2 dimers, we found that magnetic state of less stable vertical (Ru_2) and parallel (Ir_2) dimers is quenched upon the adsorption onto Mg(001). Similar behavior was previously observed for the Au_2 dimers on MgO(001): the vertical one has a singlet ground state, while parallel one has doublet ground state.[19] In the first case the non-magnetic solution is found, while for the parallel Ir_2 dimer the magnetization of 2 μ_B was found. Previously we found that for the non-metal adsorption on defect-free Mg(001) magnetization is local in character[31] and here we report the same behavior (Fig. 2).

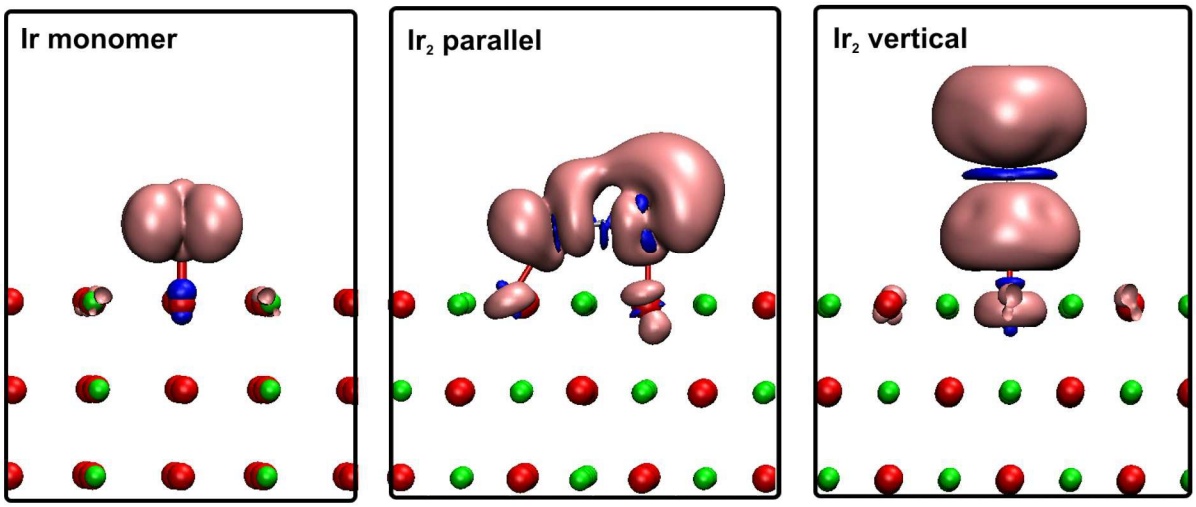

Figure 2. Distribution of spin polarization ($\rho_{\text{spin up}} - \rho_{\text{spin down}}$) for the ground states of Ir monomer and homonuclear Ir dimer adsorption on MgO(001) (the isovalues are ±0.002 e Å^{-3}).

As can be seen, the inclusion of spin polarization changes the numbers but does not change the trends of adsorption, while adsorption geometries are correctly predicted without spin-polarization approach. We further investigate the adsorption of bimetallic dimers in a combinatorial manner to observe trends in dimer adsorption, therefore, in the following spin polarization is omitted unless specifically stated otherwise.

B. Combinatorial approach to adsorption of dimers - Structures and Energetics

After the structural optimization of various initial configurations of M1M2 dimer on MgO(001) (Fig. 1) we found that the ground configuration was either a flat-OO or a vertical-O top configuration with the exception of the RuPt dimer, for which the Pt–Ru bond was shifted away from the axis perpendicular to the surface plane (Fig. 3).

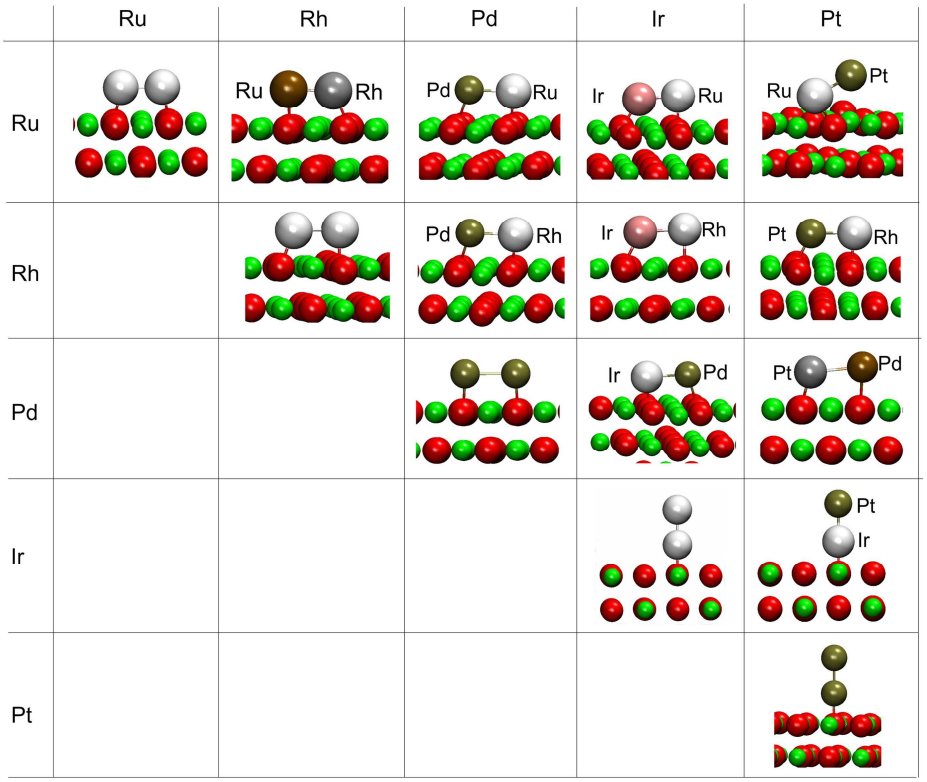

Figure 3. Optimized geometries of the ground state configurations of M1M2 bimetallic dimers on defect-free Mg(001)

The formation energy of the M1M2/MgO(001) complex was characterized by the dimer adsorption energy (E_{ads}), defined in analogous way as for homonuclear dimers:

$$E_{ads} = E_{MgO+M1M2} - \left(E_{MgO} + E_{M1M2}\right) \quad (3)$$

As defined, Eq. (3) quantifies the formation of the adsorption complex from the dimer preformed in the gas phase. There are other possibilities to quantify the dimer adsorption energy such as, for example, considering the adsorption of a M2 atom adjacent to M1 already adsorbed on MgO(001), the approach that can be used to directly estimate the dimer formation energy under growth conditions.[16] In this work we chose to quantify dimer adsorption using Eq. (3). Alternatively, one may evaluate the cohesive energy of adsorption complex (E_{coh}) as:

$$E_{coh} = E_{MgO+M1M2} - \left(E_{MgO} + E_{M1} + E_{M2}\right) \quad (4)$$

Combining Eqs. (3) and (4) one can see that E_{coh} is actually a sum of E_{ads} and the gas-phase dimer bond energy. Similar to the case of atomic adsorption, E_{ads} of dimers varies substantially. It can be noticed that the most weakly bound dimers are RuM2, as Ru itself interacts weakly with MgO(001), while E_{ads} reaches –2.08 eV for the Pd_2 dimer despite a weak interaction of the Pd atom with MgO(001) (Table 2). On the other hand, the calculated cohesive energies point to a highly exothermic formation of M1M2 dimers over the MgO surface, indicating their stability (Table 3).

Table 3. Structural and energetic parameters for dimers adsorption on defect-free MgO: calculated adsorption energies of M1M2 dimers on defect-free MgO(001) (first number), M1–M2 bond length in the dimer adsorbed on MgO(001) (second number), the change of M1–M2 bond length upon the adsorption with respect to isolated M1M2 dimer in the gas phase (third number, *italic*) and the cohesive energy of the adsorption complex (fourth number). The data reported here refer to the ground state configurations presented in Fig. 3

	Ru	**Rh**	**Pd**	**Ir**	**Pt**
Ru	−0.98 eV 2.32 Å *+0.25* Å −4.87 eV	−0.79 eV 2.35 Å *+0.19* Å −4.90	−0.92 eV 2.50 Å *+0.17* Å −3.46 eV	−0.90 eV 2.30 Å *+0.14* Å −5.76 eV	−0.98 eV[a] 2.38 Å *+0.09* Å −5.07 eV
Rh		−1.19 eV 2.38 Å *+0.18* Å −4.97 eV	−1.70 eV 2.57 Å *+0.17* Å −3.91 eV	−1.11 eV 2.38 Å *+0.17* Å −5.63 eV	−1.30 eV 2.50 Å *+0.20* Å −5.15 eV
Pd			−2.08 eV 2.82 Å *+0.24* Å −3.18 eV	−1.57 eV 2.55 Å *+0.19* Å −4.40 eV	−1.82 eV 2.72 Å *+0.33* Å −4.20 eV
Ir				−1.45 eV 2.23 Å *+0.02* Å −6.33 eV	−1.85 eV[b] 2.31 Å *0.0* Å −5.83 eV
Pt					−1.71 eV 2.38 Å *+0.02* Å −5.17 eV

[a]tilted configuration with Ru bonded directly to MgO(001). [b]vertical configuration with Ir attached to the O center of MgO(001).

We observed that E_{coh} is always lower than the sum of E_b^M of the dimer constituents. This means that the formation of a dimer is energetically favored over separate adatoms. To check this hypothesis explicitly, we have evaluated cohesive energies for monomer co-adsorption and compared them with the cohesive energies of the ground state configurations of adsorbed dimers. These calculations were performed for homonuclear dimers. If two metal atoms are placed to the adjacent O sites, upon structural relaxation they always combine to form a dimer. However, if placed at larger distances stable co-adsorbed monomers are observed (Fig. 4) with a cohesive energy which is approximately equal to the sum of corresponding E_b^M (Fig. 4).

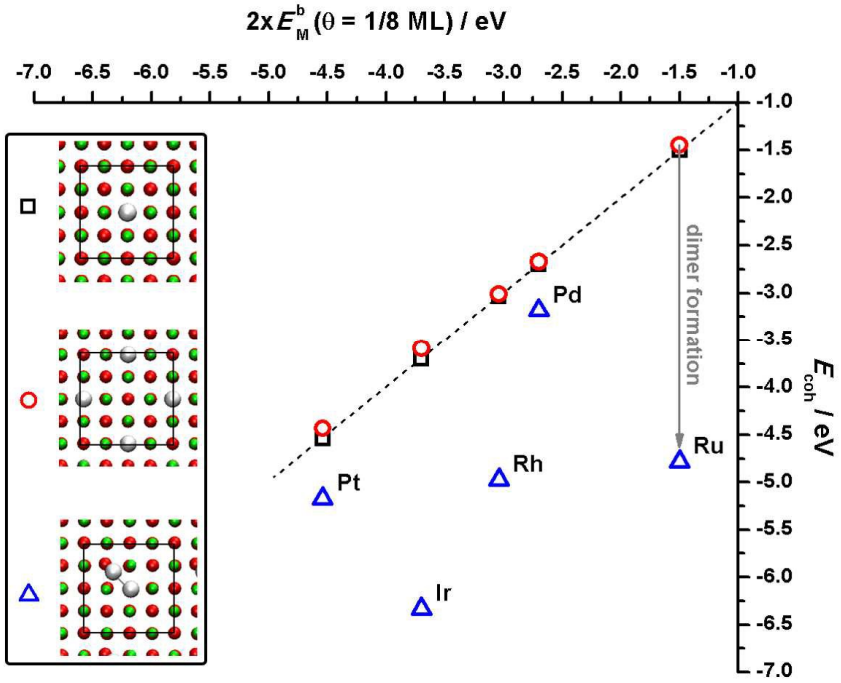

Figure 4. Cohesive energies of adsorbed homonuclear dimers (Δ) compared with the cohesive energies of co-adsorbed monomers at the same coverage by metal atoms (○). Cohesive energies for the systems with co-adsorption are practically the same as for twice lower coverage (□). If two co-adsorbed metal atoms are brought to adjacent O site dimer is formed on the surface followed by the energy gain through M–M bond formation

As a rule, we observe that the PdM2/MgO(001) adsorption complexes have the smallest cohesive energies among all M1M2/MgO adsorption complexes, which is a consequence of a weak Pd–M2 bond in the gas phase (Fig. 5). The binding energy of Pd_2 in the gas phase is evaluated to be only 1.09 eV (evaluated as the energy of homonuclear bond cleavage; bond energies reported in this work are taken positive as usually done). For comparison, the proposed benchmark Pd–Pd dissociation energy in the gas phase, obtained by *ab initio* calculations, is 0.75 eV,[47] while the experimental value[48] is (1.06±0.16) eV. Using the same methodology as applied here, Park and Yu obtained the value of 1.29 eV.[46] The binding energies of other dimers considered here are typically above 3.5 eV. Despite the fact that M1–M2 interaction is affected by the presence of MgO surface a clear correlation between E_{coh} and M1–M2 binding energy (in the gas phase) is observed (Fig. 5), which allowed us to conclude that the cohesive energy of M1M2/MgO(001) adsorption complex is dominated by the strength of the M1–M2 interaction.

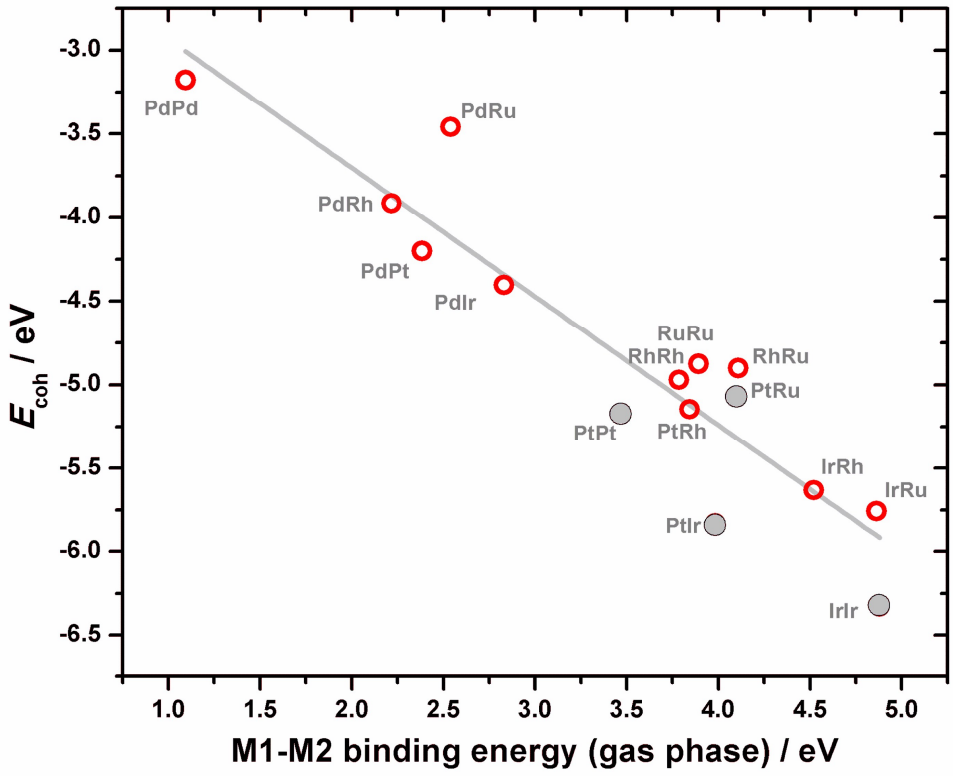

Figure 5. Cohesive energy of M1M2/MgO(001) adsorption complex (E_{coh}) as a function of M1-M2 binding energy in the gas phase. Filled circles stand for the dimers for which parallel orientation is not preferred (PtRu, PtIr, PtPt and IrIr).

We also should notice that when dimers adsorb in the parallel mode the M1–M2 bond stretches with respect to the bond length of an isolated dimer, while for dimers adsorbed vertically the change of the bond length is almost negligible (see Table 3). For example, if Pt_2 is adsorbed vertically the bond is elongated by 0.02 Å, while for the parallel orientation (less stable structure) the bond elongates by 0.18 Å. Previously it has been suggested that the bond strength in adsorbed metal dimers can be evaluated assuming that both the M–M binding energy and the M–O interaction contribution to E_{coh} (taken to be the same as for the adsorption of a single atom at the O site).[46] For the case of heteronuclear dimers, the M1–M2 bond energy (E_{M1-M2}) can be evaluated as:

$$E_{\text{M1-M2}} = -\left(E_{\text{coh}} - E_{\text{b}}^{\text{M1}}\right) \quad (5)$$

for a vertically adsorbed dimer and:

$$E_{\text{M1-M2}} = -\left(E_{\text{coh}} - \left(E_{\text{b}}^{\text{M1}} + E_{\text{b}}^{\text{M2}}\right)\right) \quad (6)$$

for a dimer adsorbed in the parallel orientation (a more positive value means a stronger bond). In Eq. (5) M1 is the metal atom in the dimer attached to the O adsorption site. Based on Eqs. (5) and (6) one can suggest that the M1–M2 bond is weaker in the dimer adsorbed parallel to the surface. For the case of Pt_2, we evaluated E_{M1-M2} to be 2.91 and 0.50 eV for vertical and parallel dimer, respectively. As a reference, the Pt–Pt bond energy of the isolated dimer is evaluated to be 3.46 eV. For comparison, Park and Yu, who used projector-augmented wave (PAW) method in combination with PBE approximation, obtained the values of 3.49 (vertical adsorption) and 0.77 eV (parallel adsorption), and also reported the binding energy of the isolated Pt–Pt dimer in

the gas phase to be 3.81 eV.[46] The value obtained from experiment for the gas phase Pt_2 is 3.14 eV,[49] while Grönbeck and Broqvist[39] calculated the same quantity to be 2.4 eV at PBE level. The weakening of the M1–M2 bond in the dimer upon its parallel adsorption is less pronounced if metals interact weakly with the O centers. For example, for the PtRh dimer we obtained the values of Pt–Rh binding energies of 3.25 and 1.35 eV for the vertical and parallel orientations, respectively, while the bond energy in the gas phase is 3.84 eV. However, if one calculates the dimer deformation energy in the gas phase when placing M1 and M2 at the distance as in the adsorbtion complex, a certain discrepancy is observed, suggesting that such an energy decomposition scheme should be taken with certain care. For the case of Pt_2 for which the Pt–Pt bond is stretched to match the one in the flat laying dimer, the bond is destabilized by only 0.22 eV. On the other hand, a similar calculation for the vertically adsorbed dimer shows that the bond energy stays virtually the same. Hence, it appears that the E_b^{M1} and E_b^{M2} terms are also affected by the presence of the second metal atom and that the interaction between the constituents of the dimer with the O centers cannot be considered independently of the interaction between the metal atoms of the dimer. This also explains a good correlation between E_{coh} and metal binding energy in the gas phase (Fig. 5). In this sense, Pd_2 is a particular case. It has the longest M–M bond and most negative E_{ads} among studied dimers (Table 3), whereas a single Pd atom interacts relatively weakly with MgO(001) (Table 1). Such a behavior can be rationalized in terms of a weak Pd–Pd bond and stronger Pd–O bond. Therefore, the Pd_2 adsorption is governed by the Pd–O interaction while Pd–Pd interaction is even weaker than in the gas phase.

The question is why some dimers prefer parallel adsorption and some vertical. The answer to this question appears simple – dimers tend to maximize cohesive energy. On the other

hand, there are many underlying factors that govern this process and many different energy contributions to the cohesive energy that cannot be decomposed in a unique way, so the definite answer about the factors that govern dimer orientation with respect to MgO surface is beyond the scope of this work. However, to approach the answer, at least qualitatively, we compare behavior of the Pt_2 and Pd_2 dimers, well documented cases in the literature,[14,39,46] when the internuclear distance is changed in the gas phase (Fig. 6). A strong Pt-Pt bond in the Pt_2 dimer does not allow large stretching (which would induce large interatomic forces) to maximize the overlap between the Pt and O electronic states. For the case of Pd_2 interatomic forces allow stretching of the dimer so that the Pd atoms can interact more directly with O centers of MgO(001) resembling more an atomic adsorption case. In this sense, the preference between vertical and parallel adsorption can be considered as results of a compromise between the tendency of metal atoms in the dimer to maximize the interaction with O adsorption centers on the surface and to maximize mutual interaction. If the deformation of a M1-M2 bond is too large to be compensated by optimal M-O interaction dimer prefers vertical adsorption. This is, of course, a rather simplified view that does not account for the charge transfer to the adsorbate (see the next Section), which is orientation-dependent and would also affect the bond strength and the interatomic forces in the adsorbed dimer.

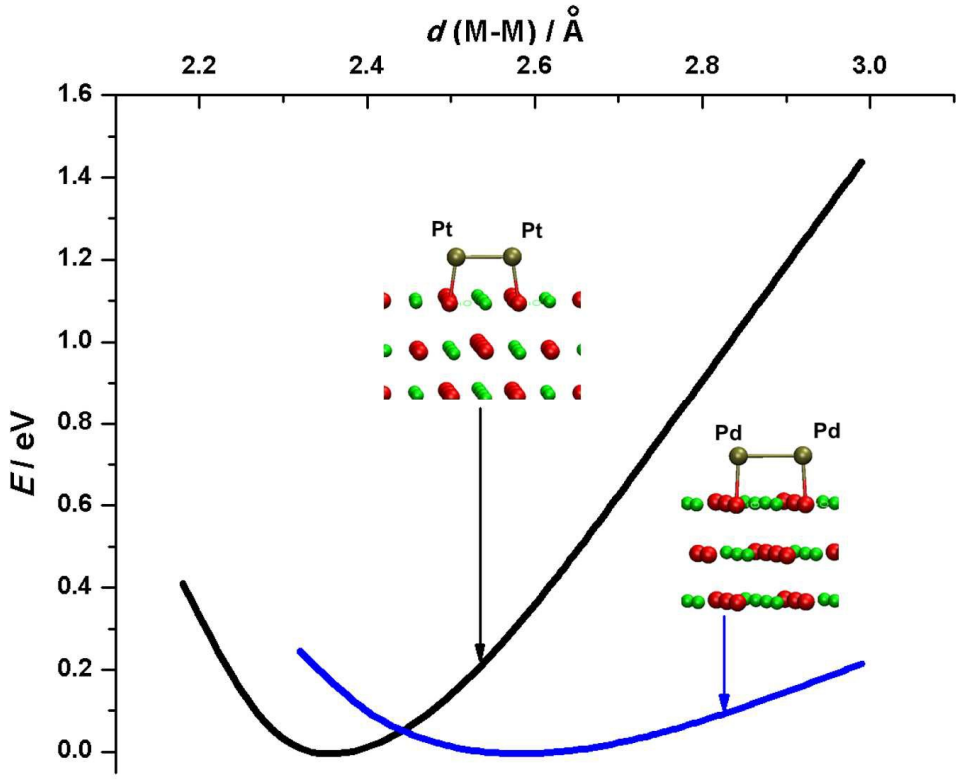

Figure 6. Potential energy as a function of internuclear distance for Pt_2 and Pd_2 bond in the gas phase (as the zero energy the dimer ground state is taken). Dimer equilibrium distance when adsorbed on MgO(001) is indicated. The curves were constructed using spin-polarized calculations with magnetization matching the one of the ground state of adsorbed dimer (Table 2)

C. Charge state and the electronic structure of dimers on MgO(001) – trends in the Periodic Table of Elements

The charge state of adsorbed metal atoms and cluster has attracted a significant attention in the field. There are many different schemes to determine the charge state of adsorbed species and usually different approaches give different results. For example, Neyman *et al.* used potential-derived charges and suggested that for the series of transition metal atoms adsorbed on

MgO(001) (including the ones investigated here) the charge transfer is very small (bellow 0.2|e|) and typically from adsorbate to substrate.[40] This observation let the authors claim that the bond between the metal adatom and MgO substrate is of a covalent nature. On the other hand, Grönbeck and Broqvist used Mulliken population analysis to show that a Pt monomer adsorbed on MgO(001) bears approximately 0.5 excess electrons (being negatively charged), gained from the surface O atom at which it is adsorbed.[39] Using the Bader analysis we observed that the net charge transfer to Pt monomer is of about 0.45|e| (Table 4). Former literature reports suggested that Pt on MgO(001) is negatively charged. For comparison, Jeon *et al.* reported that 0.39|e| is transferred to Pt adsorbed at the O site of MgO(001).[50] For the Rh/MgO(001) system and Rh coverage of 1/8 ML, previously reported spin-polarized DFT–PBE calculations suggested that 0.27|e| was transferred to the Rh adatom.[42] For the Pd/MgO(001), the Bader analysis revealed that 0.15|e| is transferred to the Pd adatom.[44] The Mulliken analysis performed by Mineva *et al.* for the Rh/MgO(001) and Pd/Mg(001) systems, investigated using spin-polarized PBE calculations, showed that Rh and Pd bear partial charges amounting to −0.27|e| and −0.25|e|, respectively.[41] The analysis of the previously published data suggests that computational scheme employed in this work correctly accounts for the charge state of adsorbed atoms on MgO(001). When spin polarization is taken into account, the Bader charges are moderately affected, as can be seen for the case of adsorbed monomers (Table 4).

Table 4. Partial charge (q, in |e|), calculated by means of Bader analysis, of M1 combined with M2 for ground configurations of M1M2 dimers adsorbed on MgO(001). Where flat geometry is not preferred one, the data for such dimer orientation are given in parentheses. For monomers, Bader charges evaluated using spin-polarized approach are included (in parentheses, italic)

q **/ |e|**	**M1**				
	Ru	**Rh**	**Pd**	**Ir**	**Pt**

	Ru	−0.23	−0.43	−0.37	−0.59	−0.82 (−0.66)
	Rh	−0.08	−0.19, −0.37[b]	−0.30	−0.53	−0.57
M2	**Pd**	−0.12	−0.23	−0.23	−0.42	−0.55
	Ir	0.00	−0.10	−0.21	−0.39[a] (−0.30, −0.45)[b]	−0.42 (−0.52)
	Pt	+0.26 (+0.05)	−0.11	−0.07	+0.02 (−0.25)	−0.27[a] (−0.34, −0.41)[b]
adsorbed monomer		−0.28 (*−0.25*)	−0.28 (*−0.25*)	−0.24 (*−0.24*)	−0.46 (*−0.44*)	−0.45 (*−0.43*)

[a]Given for the atom not attached to the surface. [b]Due to the asymmetry of a flat laying dimer charges at two atoms differ to certain amount.

Considering adsorbed monomers we observed that the 4d elements drain less charge from the MgO substrate than the 5d elements. This charge predominantly originates from the O center on which the adatom is located. As presented in Fig. 7 for the case of PdPt, the dimer adsorption induces a charge redistribution within the dimer and between the dimer and the support. More importantly, we observe that the charge state of metal atom in the adsorbed dimer is not the same as when this atom is adsorbed separately. The pattern of charge redistribution can be obtained in two ways, either considering dimer adsorption on MgO(001) from the gas phase (Fig. 7 A), or the formation of the adsorption complex from isolated metal atoms (Fig. 7 B). If we take the PtPd dimer as an example, then using both approaches we observe~~s~~ that charge gets redistributed in a way to reduce Coulombic repulsion. The electron cloud is drawn by positive Mg^{2+} centers that stabilize the formation of the adsorption complex. On the support side, adsorption induces a charge redistribution predominantly at the adsorption site including the two O centers through which the dimer binds to MgO(001).

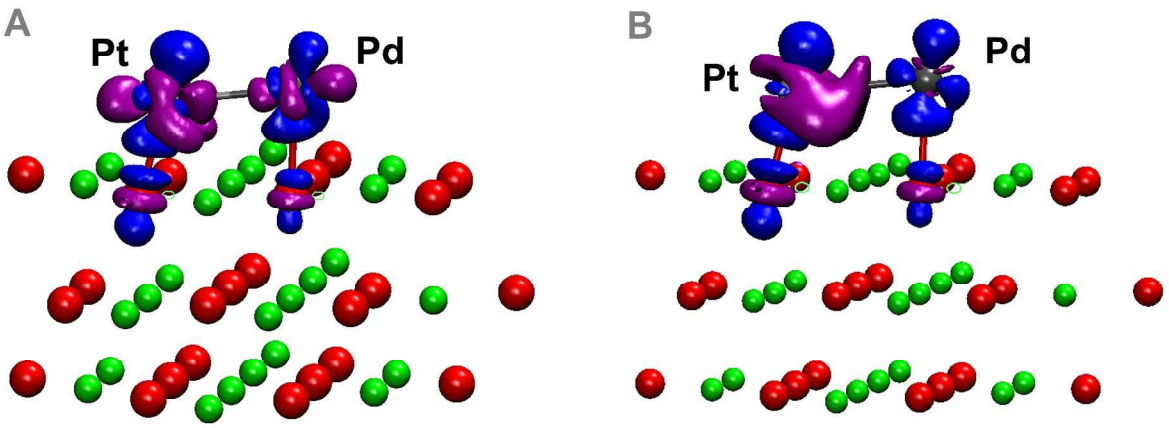

Figure 7. Charge difference plot for the case of the heteronuclear PtPd dimer adsorbed on MgO(001): A – considering the formation of PtPd+MgO(001) complex from isolated PtPd and Mg(001), B – considering the formation of the adsorption complex from isolated Pt and Pd atoms and MgO(001). The isosurface values are ±0.008 e $Å^{-3}$ (purple – build up of charge density, blue – depletion charge density). In isolated dimer Pt takes 0.2e from Pd, and becomes partially negatively charged. When adsorbed Pt bears −0.55e while Pd bears −0.07e, indicating that −0.62e are transferred into the adsorbed dimer from the substrate.

Although the analysis shows that charge redistribution is localized to the dimer and adsorption site, we performed an additional calculation with larger, 3×3, unit cell to see how the dimer–dimer distance can influence the charge transfer, as well as binding and cohesive energies and relative differences between different dimer orientations. The test showed that binding and cohesive energies were altered by less than 0.01 eV, while the calculated Bader charges differed by less than 0.015e. The calculated densities of states were virtually identical and the positions of d-band centers were unaffected by the size of the supercell.

For a M1M2 dimer of a defined orientation (flat or vertical), the partial charge of M1 becomes more negative when the position of M2 moves up and to the left in the PTE (Table 4). For the homonuclear dimers adsorbed parallel to the surface the calculated charge transfer to the dimer constituents is similar to that of the adsorbed monomers. This is consistent with previous reports

considering Pt[39] and Pd[44] dimers adsorbed on Mg(001). Notice that the charge state can be different for dimers of different orientations. So far, such differences have been observed for Au_2 on single crystal thin MgO(001) films grown on the Ag(001) substrate.[19] Using Bader analysis, the authors have shown that the energetically more stable upright Au_2 dimer is charge neutral, while the flat laying dimer is charged. In our case, Bader analysis revealed a general trend that the charge of the upright dimers is always less negative than that of flat laying ones. As an example, the flat Pt_2 dimer bears the net negative charge of 0.75|e| while the upright dimer only 0.39|e| (Pt attached to the surface has extra 0.12|e| while the topmost Pt atom has 0.27|e|). Even more interesting case is the PtIr dimer. For the flat one, Pt bears −0.52|e| while Ir bears −0.25|e|. If PtIr is adsorbed vertically with Ir attached to the surface these charges are −0.42 and +0.02|e| for Pt and Ir, respectively. In order to understand this behavior we compare the excess charges of the vertical and flat dimers and those of co-adsorbed monomers (the same metal coverage as for the dimer adsorption) with the excess charges found on adsorbed monomers (the case of homonuclear dimers, Fig. 8). In the case of co-adsorbed monomers, the excess charge *per* one metal atom is virtually the same as for adsorbed monomers, but the charge transfer to the adsorbate is large compared to adsorbed flat dimers (Fig. 8). On the other hand, the amount of charge transferred to vertical dimers is typically smaller compared to the case of monomer adsorption. Such a behavior can be understood on the basis of (i) the inability of a single O center to donate large amount of charge to the adsorbate and (ii) effective saturation of metal atoms in vertical dimers due to M–M interaction (compared to monomers and stretched flat dimers).

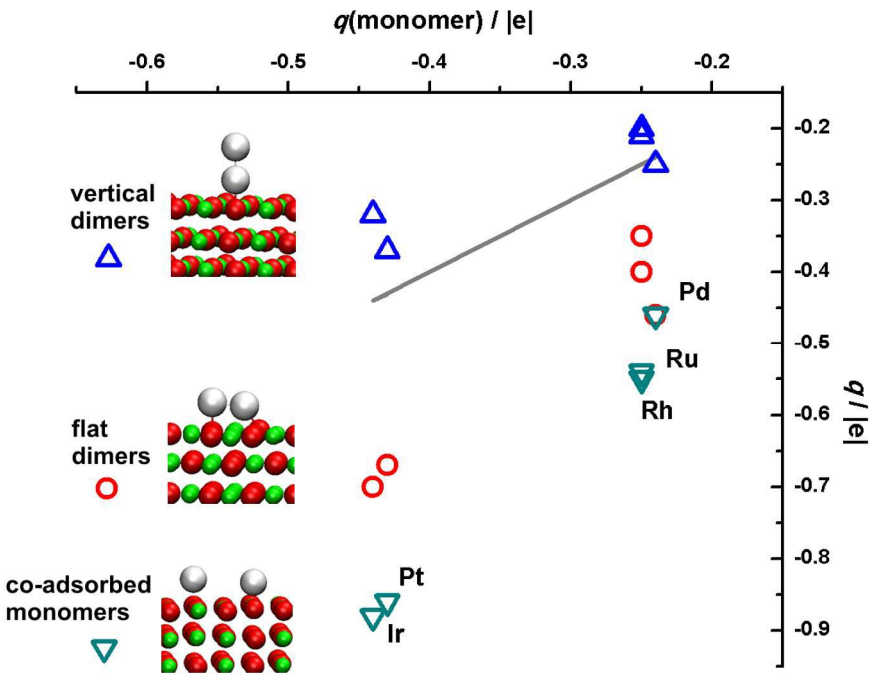

Figure 8. Bader charges found on vertical and flat dimers and co-adsorbed monomers compared to Bader charges found on monomers.

Different charge states are the first indication that one can expect different electronic structures of a particular dimer depending on its orientation. Moreover, the electronic structure will be altered compared to the monomer adsorption. Indeed, such a behavior can be seen, for example, for the Pd monomer and dimer as demonstrated in Fig. 9. In the case of the Pd adatom (Fig. 9, middle) the d states are highly localized and resemble the ones of an isolated atom. However, upon addition of another Pd atom to the adjacent O site (Fig. 9, left) or on top of pre-adsorbed Pd atom (Fig. 9, right) a significant alteration of the electronic structure takes place. A strong overlap of the d-states of the two Pd atoms is observed indicating a covalent type interaction between atoms in the dimer.

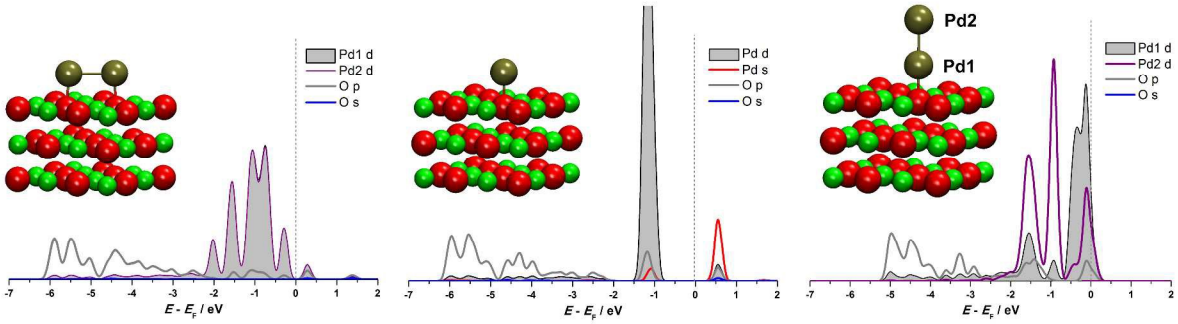

Figure 9. Projected densities of states of Pd_2 adsorbed parallel to the MgO(001) (left), adsorbed Pd atom (middle) and Pd_2 adsorbed vertically on MgO(001). For the later systems d-band centers of Pd atoms are located at −0.96 eV (Pd1) and −1.09 eV (Pd2) *vs*. Fermi level, while partial charges are −0.25 and −0.01|e|, in the same order.

Pronounced differences in the electronic structure of monomers and differently oriented dimers allow one to expect a diverse reactivity of these chemical entities. It is, however, necessary to quantify the modification of electronic structure in a comprehensive way. For this purpose the d-band center position (E_d) was selected. This was done for two reasons. First, the projected densities of states of the analyzed dimers (Fig. 9) show that the d-states of the atoms in adsorbed dimers are not localized like in molecules but get re-hybridized with the O center 2p states and delocalized in a band-like manner. Widening of the metal d-states is also due to the interaction of the atoms of the dimer. Secondly, this quantity has largely been exploited as a descriptor of the chemisorptions properties and catalytic activity of solid surfaces.[51, 52]

E_d was evaluated as a first moment of the band while only occupied states were considered. Taking a look at the values of E_d calculated for M1 in the flat lying dimers one can see that there is a clear dependence of E_d on the position of M2 in the PTE (Table 5). When M2 moves to the right along the row in the PTE E_d shifts towards higher energies (gets destabilized, Table 5). When moving down the group of the PTE the d-band center shifts to lower energies (gets stabilized, Table 5).

Table 5. Calculated *d*-band centers (in eV) of M1 combined with M2 for ground configurations of M1M2 dimers adsorbed on MgO(001). Where flat geometry is not preferred one, the data for such dimer orientation with respect to the surface plane are given in parentheses. The data for adsorbed monomers are also included

	E_d / eV	M1				
		Ru	**Rh**	**Pd**	**Ir**	**Pt**
M2	**Ru**	−1.93	−1.83	−1.90	−2.29	−1.56 (−2.23)
	Rh	−1.66	−1.55[b]	−1.58	−1.99	−1.92
	Pd	−1.42	−0.91	−1.37	−1.36	−1.70
	Ir	−1.79	−1.80	−1.61	−1.83[a] (−2.17)[b]	−1.59 (−2.11)
	Pt	−1.81 (−1.45)	−1.21	−1.31	−1.90 (−1.69)	−1.04[a] (−1.77)[b]
	monomers	−0.80	−0.83	−1.49	−0.99	−1.44

[a]Given for atom not attached to the surface. [b]Despite the differences in partial charges of atoms in flat dimer (Table 4) d-band center positions were found to be identical.

From the literature on solid surfaces it is known that E_d is modified through the strain and ligand effects.[53] An analogy can be drawn between adsorbed bimetallic dimers and solid surfaces. The formation of a strong covalent bond in the dimer would stabilize the d-band lowering E_d with respect to the Fermi level. As a rule, the strength of the M1–M2 bond decreases as M2 moves to the right along the row in the PTE and increases as it moves down the group of the PTE. The stabilizing effect due to the chemical environment changes in the same manner. If one considers the theory of chemisorption by Hammer and Nørskov,[25] one can expect that the chemisorption properties of bimetallic dimers can be modified by changing its chemical

composition. More importantly, capturing the trends of such modifications can be useful for the optimization of the catalytic properties of supported metal clusters.

D. Chemisorption properties of supported metal dimers and the link to its electronic structure

In order to probe the chemisorption properties of bimetallic dimers we concentrated on PdM2 and PtM2 dimers, while CO was chosen as a probe molecule. We notice that such structures were found to be stable and the CO molecule always remained attached to the atom at which it was initially placed. This is consistent with the previously published report where it was shown for the case of Pt_2 adsorbed parallel to the MgO surface that CO adsorbs preferentially on top of Pt but not at the bridge position between two Pt atoms. The latter configuration is, however, preferred for the case of Pt_2 in the gas phase.[39] Such a difference can be explained by the Pt-Pt bond elongation in the flat laying dimer, which does not allow CO to benefit from the interaction with both metal atoms. Therefore, CO chooses the on-top adsorption site.

CO adsorption energy (E_{ads}(CO)) was calculated as:

$$E_{ads}(\mathrm{CO}) = E_{\mathrm{MgO+M1M2+CO}} - \left(E_{\mathrm{MgO+M1M2}} + E_{\mathrm{CO}}\right) \quad (7)$$

where $E_{\mathrm{MgO+M1M2+CO}}$ and E_{CO} stand for the total energy of MgO-supported M1M2 dimer with adsorbed CO and the total energy of isolated CO molecule. E_{ads}(CO) was also calculated for supported metal monomers. For the studied MgO-supported dimers an obvious dependence of E_{ads}(CO) with respect to their chemical composition is revealed (Table 6). E_{ads}(CO) calculated for dimers of different orientations differ greatly.

CO chemisorption is described within Blyholder model as a coupling of the CO 5σ (donation) and 2π* states (backdonation) to the metal *d*-valence states.[54] With this premise, Hammer *et al.* have shown that the d-states contribution to the CO chemisorption energy ($E_{\text{d-hyb}}$) should scale with the position of the d-band center as:

$$\delta E_{\text{d-hyb}} \approx \left[-4fV_{\pi}^{2}/\left(\varepsilon_{2\pi}-E_{\text{d}}\right)\delta E_{\text{d}}\right] \quad (8)$$

where f is the fractional filling of the d bands, $\varepsilon_{2\pi}$ is the position in energy of the (renormalized) adsorbate state, and V_{π} is the coupling matrix.[55] This model is widely exploited to investigate chemisorptions properties of solid surfaces. However, the underlying physical reasoning does not restrict this model to be applied to any of d metal containing systems where d-states have a band-like character. If CO chemisorption energies at the Pt (Pd) atoms in PtM2 (PdM2) dimers (Table 6) are correlated with the calculated positions of d-band centers (Table 5) one obtains a clear linear correlation, splitting for parallel and vertically adsorbed dimers. However, the trend is similar for the two adsorption modes and it confirms what we know about solid surfaces: the chemisorption becomes stronger as d-band center shifts towards the Fermi level (Fig. 10).

Table 6. CO adsorption energies and C−O and C−M bond lengths (in angstroms) for investigated PdM and PtM dimers. Data for CO adsorption on Pd and Pt monomers on MgO(001) are also included, along with CO chemisorption energies on Pd(111) and Pt(111) surfaces. For the dimer configurations not being preferential ones data are given in *italic*. For the isolated CO bond length was found to be 1.14 Å. Literature data are given in square brackets.

dimer (orientation)	E_{ads}(CO) / eV	*d*(C−O) / Å	*d*(C−M) / Å
PdRu (parallel)	−1.93	1.16	1.87
PdRh (parallel)	−2.14	1.16	1.87
PdPd (parallel)	−2.46	1.16	1.86
PdIr (parallel)	−2.02	1.16	1.88
PdPt (parallel)	−2.47	1.16	1.86

PdPd (vertical)	*−1.61*	*1.16*	*1.90*
IrPd (vertical)	*−1.06*	*1.16*	*2.00*
PtPd (vertical)	*−1.28*	*1.16*	*1.98*
Pd monomer	−2.49 [−2.63][a]	1.16 [1.164][a]	1.87 [1.845][a]
Pd(111)	[−1.247; −1.602][b]		
PtRu (parallel)	*−2.64*	*1.17*	*1.83*
PtRh (parallel)	−3.02	1.17	1.83
PtPd (parallel)	−3.53	1.17	1.82
PtIr (parallel)	*−2.91*	*1.17*	*1.83*
PtPt (parallel)	*−3.61* [−3.67][c]	*1.17* [1.18][c]	*1.82* [1.83][c]
PtRu (tilted)	−2.46	1.17	1.83
PtIr (vertical)	−2.33	1.17	1.85
PtPt (vertical)	−2.82	1.17	1.81
Pt monomer	−3.63 [−3.57][b]	1.17	1.80
Pt(111)	[−1.48][d]	[1.15][d]	[1.88][d]

[a]Reference.[56] [b]Reference.[57]; the first number for on top adsorption, the second one for hcp adsorption site (experimentally found as preferred). [c]Reference.[39] [d]Reference.[58]; on top adsorption (experimentally found as preferred).

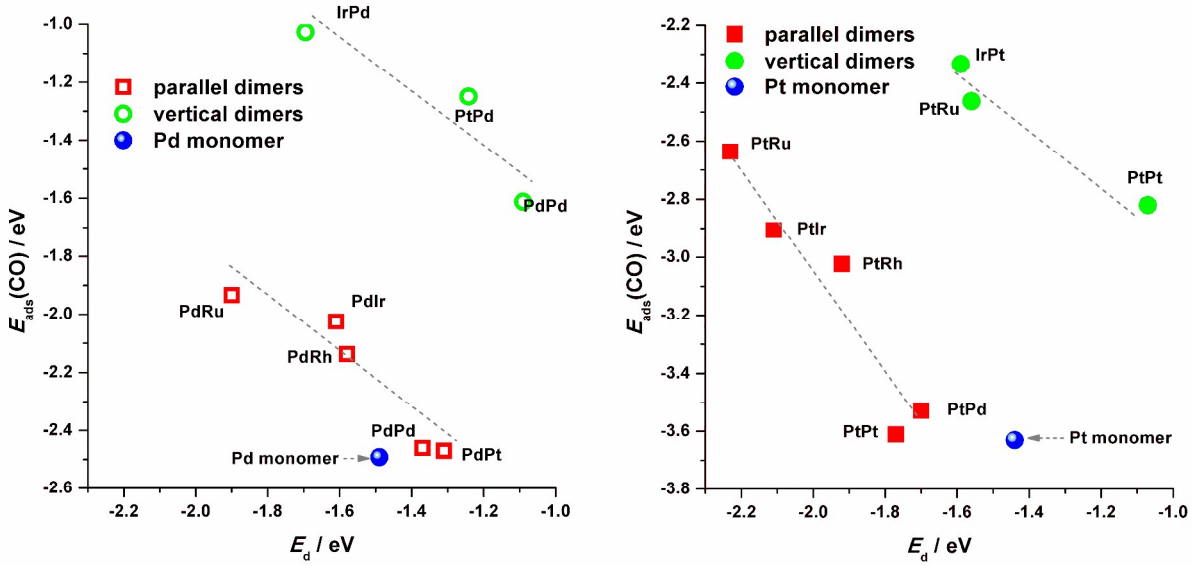

Figure 10. Correlation between CO adsorption energy (E_{ads}(CO)) on Pd (left) and Pt (right) atoms in MgO(001)-supported PdM or PtM dimers with the position of the corresponding d-band center

(E_d). Vertical M1Pd dimers are attached to MgO(001) with M1-end. For "vertical" PtRu initial configuration is the preferential one (see Fig. 3). Data for CO adsorption on Pd and Pt monomers are also included.

By analyzing Eq. (8) one can predict that for Pt and Pd based systems the slope of E_{ads}(CO) *vs*. E_d should be steeper for the Pt-based ones as the coupling matrix dominates the slope and it is significantly larger for Pt.[59] Hence, CO adsorption should be more sensitive to the E_d shift on the Pt atoms of Pt-containing dimers, as one also can see from Fig. 10.

Two aspects of CO chemisorption on the studied dimers should be mentioned. First, there is quite a large difference between the Pt–CO and Pd–CO bond strengths in these dimers. This difference is also found for the CO interaction with the Pd(111) and Pt(111) surfaces as well as with isolated Pd and Pt atoms. The literature data show that the on-top interaction of CO is weaker for Pd(111) than for Pt(111) surface (Table 6). Also, for the CO interaction with an isolated Pt atom we obtained the bond energy of 3.42 eV, while for Pd–CO bond energy the value was 2.24 eV. This means that the properties of the atoms of the flat laying dimers are close to those of an isolated atom although modified by the presence of the adjacent second atom in the dimer and the support (as seen through the modification of E_d, see Table 5). A stronger bonding of CO to Pt or Pd monomer supported by a substrate as compared to Pt and Pd (111) surfaces is clearly due to the under-coordination of the monomers. On the other hand, a stronger Pt–CO interaction, compared to the Pd-CO case, can be rationalized in terms of the model of Hammer *et al.*[55] as a hindered 5σ→d donation due to the higher fractional filling of Pd d-states, compared to Pt. This is also seen in the larger Pd–C distance, compared to the Pt–C distance, when CO is adsorbed on MgO-supported dimers. Therefore, in the case of flat laying dimers, the CO interaction with Pd(Pt) atom is mainly as for an adsorbed monomer being weakened by the presence of adjacent M2 atom as it saturates Pd(Pt) dangling bonds. Such a view is supported by

the analysis of the electronic structure of CO adsorbed on flat laying Pd_2 and supported Pd monomer (Fig. 11). In both cases the Pd d-states shift down to lower energies indicating a strong covalent interaction of the Pd d-states with CO states. For Pd_2 in the gas phase we have evaluated the Pd–CO bond energy to be 1.87 eV, while bonding of CO to Pt_2 in the gas phase on top of one of the Pt atoms amounts to 2.25 eV. When a dimer is adsorbed in vertically at the O top site of MgO(001) the bond length changes very little (in contrast to the flat laying dimer, Section B), and its chemisorptions properties remain similar as in gas phase.

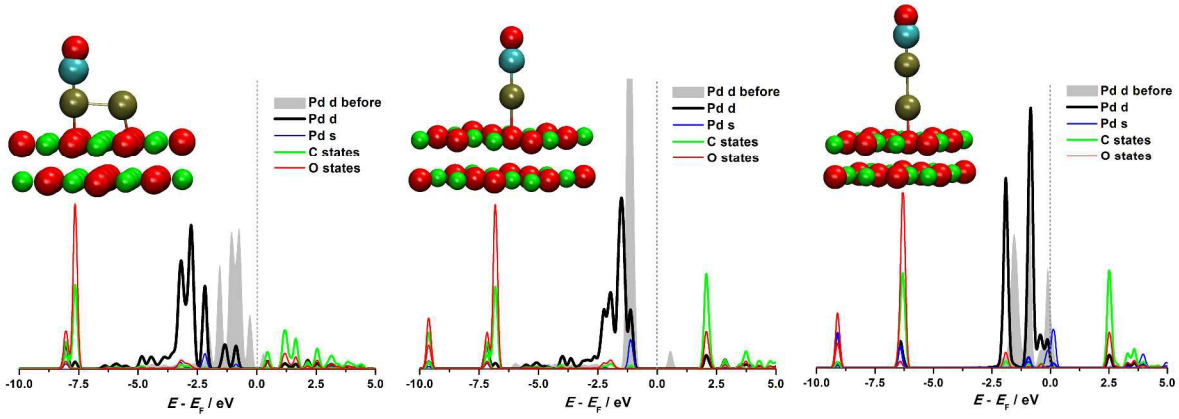

Figure 11. Projected density of states of C and O atoms of CO molecule and reactive Pd atom in Pd dimers and monomer upon CO adsorption. For comparison, corresponding projected density of d states before adsorption is also provided. Inset give optimized structures of CO adsorbed on Pd dimers and monomer attached to MgO(001).

Connecting the presented results to real catalysis one could recall the work of Qiao *et al.* who have shown that the improved CO oxidation activity of single Pt atoms supported on FeO_x is due to the weakened Pt–CO interaction resulting in low catalyst poisoning.[3] Thus the tuning of the chemical composition of a supported metal dimer could be employed to optimize the performance for a particular catalytic process. It is important to note that in the case of solid

surfaces there are well established electronic structure-related descriptors, which enable the prediction of surface reactivity.[51,53] In the case of under-coordinated supported metal clusters, however, such descriptors are missing. The results presented here (Fig. 10) offer a clue for the understanding of the trends in the reactivity of supported metal clusters based on the electronic structure of the system.

Finally, we want to point out one particular consequence of different CO chemisorption properties of differently oriented dimers. For all the Pd-based dimers the preferred geometry is the flat and the CO chemisorption does not change their orientation. However, for Pt-based dimers, Pt_2 and PtIr dimer prefer to adsorb vertically. However, a significant gain in energy upon CO adsorption stabilizes the dimer oriented parallel to the surface. For Pt_2 under CO chemisorption conditions the flat structure becomes more stable than the vertical one by 0.74 eV, while for PtIr this difference is 0.38 eV. Hence, chemisorption properties, which could be observed experimentally, might be different from those expected on the basis of theoretical calculations if such a structural rearrangement is not taken into account. In more general terms, the adsorption-induced changes of catalytically active particles can significantly affect catalyst performance and, therefore, should be considered.

IV. Conclusions

In the present contribution a systematic DFT-GGA study of M1M2 metal dimers (M1, M2 = Ru, Rh, Pd, Ir, Pt) supported on defect free MgO(001) was conducted. It was observed that the charge state and electronic structure of atoms in dimers greatly depend on the composition of a particular dimer and the position of the elements in the Periodic Table of Elements. Charge transfer from MgO to M1 in a M1M2 dimer decreases as M2 moves down and to the right in the

PTE. A clear linear relationship between the CO adsorption energy and the position of the d-band center of Pt and Pd atoms in PtM2 and PdM2 dimers was observed, allowing us to extend the applicability of the d-band center model to supported metal clusters.

Acknowledgements

This work was funded by Swedish Research Council through the project "Catalysis by metal clusters supported by complex oxide substrates". SNIC is acknowledged for providing computational time.

References

1 U. Heiz and E. L. Bullock, *J. Mater. Chem.*, 2004, **14**, 564-577.

2 I. N. Remediakis, N. Lopez and J. K. Nørskov, *Angew. Chem. Int. Ed.*, 2005, **44**, 1824-1826.

3 B. Qiao, A. Wang, X. Yang, L. F. Allard, Z. Jiang, Y. Cui, J. Liu, J. Li and T. Zhang, *Nat Chem*, 2011, **3**, 634-641.

4 S. Muratsugu, Z. Weng, H. Nakai, K. Isobe, Y. Kushida, T. Sasaki and M. Tada, *Phys. Chem. Chem. Phys.*, 2012, **14**, 16023-16031.

5 D. Yardimci, P. Serna and B. C. Gates, *Chem. Eur. J.*, 2013, **19**, 1235-1245.

6 M. Amft and N. V. Skorodumova, *Phys. Rev. B*, 2010, **81**, 195443.

7 B. Yoon, H. Häkkinen, U. Landman, A. S. Wörz, J.-M. Antonietti, S. Abbet, K. Judai and U. Heiz, *Science*, 2005, **307**, 403-407.

8 F. Frusteri, S. Freni, L. Spadaro, V. Chiodo, G. Bonura, S. Donato and S. Cavallaro, *Catal. Commun.*, 2004, **5**, 611-615.

9 F. Frusteri, S. Freni, V. Chiodo, L. Spadaro, O. Di Blasi, G. Bonura and S. Cavallaro, *Appl. Catal., A*, 2004, **270**, 1-7.

10 M. Ménétrey, A. Markovits and C. Minot, *Surf. Sci.*, 2004, **566–568, Part 2**, 693-697.

11 N. V. Skorodumova, K. Hermansson and B. Johansson, *Phys. Rev. B*, 2005, **72**, 125414.

12 C. Inntam, L. V. Moskaleva, K. M. Neyman, V. A. Nasluzov and N. Rösch, *Appl. Phys. A*, 2006, **82**, 181-189.

13 M. Sterrer, M. Yulikov, E. Fischbach, M. Heyde, H.-P. Rust, G. Pacchioni, T. Risse and H.-J. Freund, *Angew. Chem. Int. Ed.*, 2006, **45**, 2630-2632.

14 M. Sterrer, T. Risse, L. Giordano, M. Heyde, N. Nilius, H.-P. Rust, G. Pacchioni and H.-J. Freund, *Angew. Chem. Int. Ed.*, 2007, **46**, 8703-8706.

15 A. M. Ferrari, C. Xiao, K. M. Neyman, G. Pacchioni and N. Rosch, *Phys. Chem. Chem. Phys.*, 1999, **1**, 4655-4661.

16 L. Giordano, C. Di Valentin, J. Goniakowski and G. Pacchioni, *Phys. Rev. Lett.*, 2004, **92**, 096105.

17 V. Musolino, A. Selloni and R. Car, *Phys. Rev. Lett.*, 1999, **83**, 3242-3245.

18 L. Xu, G. Henkelman, C. T. Campbell and H. Jónsson, *Phys. Rev. Lett.*, 2005, **95**, 146103.

19 V. Simic-Milosevic, M. Heyde, N. Nilius, T. König, H. P. Rust, M. Sterrer, T. Risse, H. J. Freund, L. Giordano and G. Pacchioni, *J. Am. Chem. Soc.*, 2008, **130**, 7814-7815.

20 M. Watanabe and S. Motoo, *J. Electroanal. Chem. Interfacial Electrochem.*, 1975, **60**, 267-273.

21 P. Matczak, *Surf. Rev. Lett.*, 2012, **19**, 1250035.

22 E. Florez, F. Mondragon and F. Illas, *Surf. Sci.*, 2012, **606**, 1010-1018.

23 S. Sicolo and G. Pacchioni, *Phys. Chem. Chem. Phys.*, 2010, **12**, 6352-6356.

24 G. Barcaro and A. Fortunelli, *Faraday Discuss.*, 2008, **138**, 37-47.

25 B. Hammer and J. K. Nørskov, *Surf. Sci.*, 1995, **343**, 211-220.

26 J. P. Perdew, K. Burke and M. Ernzerhof, *Phys. Rev. Lett.*, 1996, **77**, 3865-3868.

27 G. Paolo, B. Stefano, B. Nicola, C. Matteo, C. Roberto, C. Carlo, C. Davide, L. C. Guido, C. Matteo, D. Ismaila, C. Andrea Dal, G. Stefano de, F. Stefano, F. Guido, G. Ralph, G. Uwe, G. Christos, K. Anton, L. Michele, M.-S. Layla, M. Nicola, M. Francesco, M. Riccardo, P. Stefano, P. Alfredo, P. Lorenzo, S. Carlo, S. Sandro, S. Gabriele, P. S. Ari, S. Alexander, U. Paolo and M. W. Renata, *J. Phys.: Condens. Matter*, 2009, **21**, 395502.

28 R. W. G. Wyckoff, *Crystal structures*, Interscience Publishers, New York, 1963.

29 H. J. Monkhorst and J. D. Pack, *Phys. Rev. B*, 1976, **13**, 5188-5192.

30 L. Bengtsson, *Phys. Rev. B*, 1999, **59**, 12301-12304.

31 I. A. Pašti, M. Baljozović, N. V. Skorodumova, *Surf. Sci.* 2015, **632**, 39–49.

32 W. Humphrey, A. Dalke, K. Schulten, *J. Mol. Graphics*, 1996, **14**, 33-38.

33 M. Amft, N. V. Skorodumova, 2011, arXiv:1108.4669v1

34 L. M. Molina, B. Hammer, *Phys. Rev. Lett.*, 2013, **90**, 206102.

35 L. M. Molina, B. Hammer, *Phys. Rev. B*, 2004, **69**, 155424.

36 I. A. Pašti, N. V. Skorodumova, S. V. Mentus, *React. Kinet. Mech. Cat.*, 2014, doi: 10.1007/s11144-014-0808-x

37 R. F. W. Bader, *Atoms in Molecules: A Quantum Theory*, Oxford University Press, 1990.

38 G. Henkelman, A. Arnaldsson and H. Jónsson, *Comput. Mater. Sci.*, 2006, **36**, 354-360.

39 H. Grönbeck and P. Broqvist, *J. Chem. Phys.*, 2003, **119**, 3896-3904.

40 K. M. Neyman, C. Inntam, V. A. Nasluzov, R. Kosarev and N. Rösch, *Appl. Phys. A*, 2004, **78**, 823-828.

41 T. Mineva, V. Alexiev, C. Lacaze-Dufaure, E. Sicilia, C. Mijoule and N. Russo, *J. Mol. Struct.: THEOCHEM*, 2009, **903**, 59-66.

42 C. W. M. Castleton, S. Nokbin and K. Hermansson, *J. Phys.: Conf. Ser.*, 2008, **100**, 082027.

43 J. Park and B. D. Yu, *J. Korean Phys. Soc.*, 2008, 53, 1976-1981.

44 L. Xu, G. Henkelman, C. T. Campbell and H. Jónsson, *Surf. Sci.*, 2006, **600**, 1351-1362.

45 A. Bogicevic and D. R. Jennison, *Surf. Sci.*, 1999, **437**, L741-L747.

46 J. Park and B. D. Yu, *J. Phys. Soc. Jpn.*, 2010, **79**, 074718.

47 N. E. Schultz, B. F. Gherman, C. J. Cramer and D. G. Truhlar, *J. Phys. Chem. B*, 2006, **110**, 24030-24046.

48 I. Shim and K. A. Gingerich, *J. Chem. Phys.*, 1984, **80**, 5107-5119.

49 S. Taylor, G. W. Lemire, Y. M. Hamrick, Z. Fu and M. D. Morse, *J. Chem. Phys.*, 1988, **89**, 5517-5523.

50 J. Jeon, A. Soon, J. Park, S. Hong, K. Cho and B. D. Yu, *J. Phys. Soc. Jpn.*, 2013, **82**, 034603.

51 J. K. Nørskov, F. Abild-Pedersen, F. Studt and T. Bligaard, *Proc. Natl. Acad. Sci. U. S. A.*, 2011, **108**, 937-943.

52 V. R. Stamenkovic, B. Fowler, B. S. Mun, G. Wang, P. N. Ross, C. A. Lucas and N. M. Marković, *Science*, 2007, **315**, 493-497.

53 J. R. Kitchin, J. K. Nørskov, M. A. Barteau and J. Chen, *Phys. Rev. Lett.*, 2004, **93**, 156801.

54 G. Blyholder, *J. Phys. Chem.*, 1964, **68**, 2772-2777.

55 B. Hammer, Y. Morikawa and J. K. Nørskov, *Phys. Rev. Lett.*, 1996, **76**, 2141-2144.

56 A. Del Vitto, L. Giordano, G. Pacchioni and U. Heiz, *J. Phys. Chem. B*, 2005, **109**, 3416-3422.

57 S. E. Mason, I. Grinberg and A. M. Rappe, *Phys. Rev. B*, 2004, **69**, 161401.

58 I. Pašti and S. Mentus, *Phys. Chem. Chem. Phys.*, 2009, **11**, 6225-6233.

59 A. Ruban, B. Hammer, P. Stoltze, H. L. Skriver and J. K. Nørskov, *J. Mol. Catal. A: Chem.*, 1997, **115**, 421-429.